Title
Adiabatic and nonadiabatic nanofocusing of plasmons by tapered gap plasmon waveguides

Journal
Applied Physics Letters, 89(4)

ISSN
0003-6951

Authors
Pile, DFP
Gramotnev, D K

Publication Date
2006-07-01

Peer reviewed

Adiabatic and nonadiabatic nanofocusing of plasmons by tapered gap plasmon waveguides

D. F. P. Pile[a)]
Department of Optical Science and Technology, Faculty of Engineering, The University of Tokushima, Minamijosanjima 2-1, Tokushima 770-8506, Japan

D. K. Gramotnev[b)]
Applied Optics Program, School of Physical and Chemical Sciences, Queensland University of Technology, G.P.O. Box 2434, Brisbane QLD 4001, Australia

(Received 12 March 2006; accepted 4 June 2006; published online 25 July 2006)

Adiabatic and nonadiabatic nanofocusing of plasmons in tapered gap plasmon waveguides is analyzed using the finite-difference time-domain algorithm. Optimal adaptors between two different subwavelength waveguides and conditions for maximal local field enhancement are determined, investigated, and explained on the basis of dissipative and reflective losses in the taper. Nanofocusing of plasmons into a gap of ~1 nm width with more than 20 times increase in the plasmon energy density is demonstrated in a silver-vacuum taper of ~1 μm long. Comparison with the approximate theory based on the geometrical optics approximation is conducted. © *2006 American Institute of Physics*. [DOI: 10.1063/1.2236219]

Localized plasmons in metallic nanostructures offer unique opportunities for nanoscale miniaturization and integration of optical waveguides, devices and circuits,[1–7] high-resolution near-field optical microscopy[8] and lithography,[9] surface enhanced Raman scattering allowing single-molecule detection,[10–14] etc. Therefore, the ability to effectively deliver electromagnetic radiation to the nanoscale is one of the major directions of research in nano-optics.

This problem is usually solved by means of nanofocusing of light in metallic nanostructures.[15–19] For example, nanofocusing of strongly localized plasmons by sharp metallic tips and grooves was considered in the geometrical optics (i.e., adiabatic) approximation (GOA), demonstrating the possibility of effective localization (focusing) of the strongly enhanced plasmon field into nanoscale regions with dimensions as small as several nanometers.[18,19]

However, GOA is applicable only if the plasmon wave vector does not change significantly within one wavelength in the structure, i.e., at sufficiently small taper angles θ.[18,19] At these angles, the plasmon does not experience noticeable reflections in the focusing structure, and its local dispersion and field distribution can approximately be determined at every distance from the tip of the groove/metal cone, assuming that the taper angle is zero.[18,19]

While the approximate methods are straightforward, physically intuitive, and yield important conclusions about plasmon nanofocusing, small taper angles are difficult to fabricate, and they result in relatively long structures/devices. This may lead to significant dissipative losses in the metal structure. Increasing taper angle decreases distances the plasmon travels along the taper during nanofocusing, but may also lead to breaching the condition of the adiabatic regime.[18,19] This may result in noticeable reflections of the plasmon as it propagates towards the tip of the groove/metal cone. Therefore, on the one hand, increasing taper angle should lead to decreasing dissipation and increasing local field enhancement (efficiency of nanofocusing). On the other hand, increasing taper angle should result in increasing reflections of the plasmon. This should lead to increased reflective losses of the plasmon energy, decreasing local field enhancement and efficiency of nanofocusing. The competition of these opposing mechanisms may result in an optimal taper angle (for fixed wavelength and parameters of the media in contact).

Recently there has been significant interest in using gap plasmon waveguides for subwavelength nano-optical applications with subwavelength localization provided in one dimension[20,21] or even both[22–24] dimensions normal to the direction of propagation. Therefore, in this letter, we conduct rigorous numerical analysis of nanofocusing of plasmons in tapered gap waveguides in both the adiabatic and nonadiabatic regimes and determine the optimum conditions for maximally effective focusing with the strongest local field enhancement. An optimal adaptor between two subwavelength plasmonic waveguides is also suggested and analyzed. Numerical confirmation of the previously developed approximate method,[19] its applicability conditions, and accuracy are presented and discussed.

The analyzed structure is shown in Fig. 1. A vacuum gap between two silver halfspaces is tapered from an initial gap width $w_i=\lambda_{vac}/2=316.4$ nm (where $\lambda_{vac}=632.8$ nm is the vacuum wavelength for the He–Ne laser) to a final gap width $w_f=\lambda_{vac}/400=1.512$ nm with the taper angle θ. The final gap width is taken as the minimal width for which the approximation of continuous electrodynamics and the local Drude model for the determination of the metal permittivity are still approximately valid.[19,25,26] The structure is assumed to be uniform and infinite in the z direction (the system of coordinates is presented in Fig. 1).

A metallic gap can support two different types of coupled plasmon modes—with the symmetric and antisymmetric distributions of the magnetic field across the gap. However, only the symmetric gap plasmon can exist at an arbitrarily small gap width. Its wave number and localization increase with decreasing gap width, while the wave number (and effective permittivity) of the antisymmetric gap plas-

[a)]Present address: 5130 Etcheverry Hall, NSF Nanoscale Science and Engineering Center, University of California, Berkeley, CA 94720-1740; electronic mail: d.pile@berkeley.edu
[b)]Electronic mail: d.gramotnev@qut.edu.au

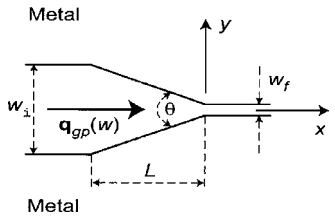

FIG. 1. The geometry of the tapered gap between two metallic media. $\mathbf{q}_{gp}(w)$ is the wave vector of the gap plasmon generated by a line source (parallel to the z axis) of a magnetic field component in the z axis located near the edge of the computational window in the wide gap section. This structure also represents an adaptor between two gap plasmon waveguides of the widths w_i and w_f. The length of the taper L is determined by the taper angle θ.

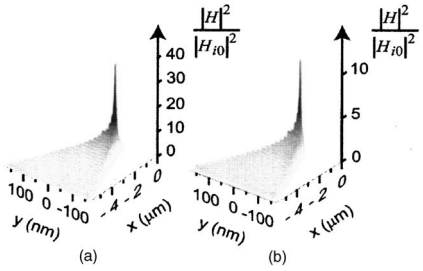

FIG. 2. The typical instantaneous (x,y) dependencies of the relative square of the magnetic field $|H|^2/|H_{i0}|^2$ in the plasmon inside the silver-vacuum taper at the vacuum wavelength $\lambda_{vac}=632.8$ nm (He–Ne laser), $w_i=316.4$ nm, $w_f=1.512$ nm, $\theta=3.24°$, and H_{i0} is the initial amplitude of the magnetic field in the plasmon at $x=-L$. (a) Dissipation in the metal is assumed to be zero: $\varepsilon_m=-16.2$. (b) Dissipation is nonzero: $\varepsilon_m=-16.2+0.5i$.

mon reduces to zero at a critical gap width and then becomes imaginary (below the critical width). Therefore, only symmetric gap plasmons can experience effective nanofocusing.[19]

A symmetric gap plasmon with the wave vector $\mathbf{q}_{gp}(w)$, where w is the varying width of the gap, propagates in the direction of the taper (i.e., along the x axis—Fig. 1). This is equivalent to the geometry of normal incidence of the plasmon focused by a V groove.[19] In this case, we can use the two-dimensional (2D) finite-difference time-domain (FDTD) algorithm for the analysis of nanofocusing. If the incident plasmon propagates at a nonzero angle with respect to the direction of the taper, then three-dimensional FDTD should be used instead, which will require substantial computational resources and will not allow analysis of nanofocusing within significant propagation distances. Therefore, the analysis in this letter is limited to the case of normal plasmon incidence (Fig. 1).

The 2D FDTD algorithm is based on the local Drude model to allow for the negative permittivity of the metal.[27] First-order Mur-type boundary conditions are used at the edges of the computational window.[28] The dimensions of the computation grid cells are $\Delta x=\lambda_{vac}/120$ and $\Delta y=\lambda_{vac}/4{,}000$.

In the FDTD simulations, the symmetric gap plasmon was excited using a line source of the electromagnetic field, parallel to the z axis, with TM polarization (magnetic field along the z axis), located near the edge of the computational window in the wide section of the gap with the width w_i. As the gap plasmon propagates into the taper, its wave number q_{gp} increases together with increasing localization of the plasmons in the y direction. This means effective focusing of the incident plasmon into the region of the width that is of the order of w_f (far beyond the diffraction limit). The tapered nanogap (Fig. 1) is analogous to a cylindrical lens, though with much tighter focusing of electromagnetic energy to a very narrow region with a possibility of a significant enhancement of the local field (see also Ref. 19). In addition, the considered structure (Fig. 1) represents an adaptor between two subwavelength gap plasmon waveguides of strongly different widths. The analysis and optimization of such an adaptor are important for the development of plasmonic circuits, interconnectors, and nano-optical devices.

Figure 2(a) presents the typical FDTD (x,y) dependence of the square of the normalized magnitude of the magnetic field $|H|^2/|H_{i0}|^2$ in the gap plasmon, where H_{i0} is the initial amplitude of the magnetic field in the plasmon at the beginning of the taper (i.e., at $x=-L$ in Fig. 1). The dissipation in the silver is assumed to be zero (i.e., $\varepsilon_m=-16.2$ with the zero imaginary part), the taper angle $\theta=3.24°$ [corresponding to change in gap width per wavelength (632.8 nm) in vacuum along the x axis of ≈ -35 nm], and the corresponding length of the taper $L\approx 5.6$ μm. In particular, it can be seen that substantial plasmon localization simultaneously with the strong local field enhancement is achieved in the structure. For example, an ≈ 31.2 times increase of the energy density in the plasmon at the narrowest part of the taper (at $x=0$) is achieved [Fig. 2(a)]. For $x>0$, the amplitude of the gap plasmon is independent of x because $w=w_f=$const (recall that the dissipation is assumed to be zero).

Using GOA (Ref. 19) for the analysis of nanofocusing in the same silver-vacuum tapered gap gives the increase in the field intensity of ≈ 31.9 times, which is only $\sim 2\%$ different from the FDTD result. This is in agreement with the expectation that the GOA approach provides good accuracy for the analysis of plasmon nanofocusing, if the taper angle θ is smaller than the critical angle $\theta_{c1}\approx 7°$, which determines the applicability of GOA in the considered structure.[19]

The effect of dissipation in the metal on nanofocusing is illustrated by Fig. 2(b), for which we assume that $\varepsilon_m=-16.2+0.5i$. As a result, the energy density increase within the taper of ≈ 11.8 times has been obtained using FDTD simulations [Fig. 2(b)], which is significantly below the enhancement achieved in Fig. 2(a). This reduction in the increase of the plasmon energy density is due to dissipative losses in the metal. GOA gives the increase of the plasmon energy density in the same structure ($\theta=3.24°$ with dissipation) of ≈ 9.0 times. The main reason for the discrepancies between the FDTD and GOA approaches for very small taper angles is due to the accumulation of numerical errors in the FDTD method. This is related to relatively large distances of plasmon propagation along the sharp taper (in the above example, $L\approx 5.6$ μm), and this results in a very large number of time iterations.

Therefore, analysis of plasmon nanofocusing in structures with small taper angles (significantly below θ_{c1}) should rather be conducted using the approximate GOA approach that provides high accuracy of results. FDTD method is inefficient in this case and may result in noticeable numerical errors. At the same time, as mentioned above, this situation is associated with significant dissipative losses for the focused plasmons, because they have to propagate large distances along the taper. Increasing taper angle decreases dissipation, but eventually causes breaching the GOA applicability condition, and the numerical approaches become essential. Fortunately, numerical errors associated with large number of time iterations reduce with increasing taper angle, which

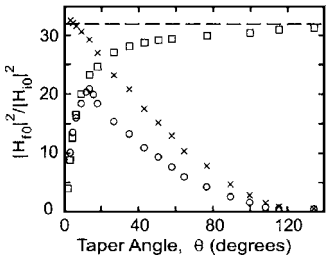

FIG. 3. The dependencies of the square of the relative plasmon amplitude $|H_{f0}|^2/|H_{i0}|^2$ at the end of the taper (i.e., at $x=0$—Fig. 1) on taper angle θ, calculated using FDTD (circles and crosses) and GOA (dashed curve and squares) in the absence of dissipation (crosses and dashed line: $\varepsilon_m=-16.2$) and with dissipation in silver (squares and circles: $\varepsilon_m=-16.2+0.5i$). The other structural and wave parameters are the same as for Fig. 2.

makes the FDTD approach increasingly more efficient. From this point of view, FDTD and GOA appear to complement each other, covering the whole possible range of taper angles.

More detailed comparison of the GOA and FDTD approaches is presented in Fig. 3 that shows the dependencies of the square of the relative plasmon amplitude $|H_{f0}|^2/|H_{i0}|^2$ at the end of the taper (i.e., at $x=0$—Fig. 1) on angle θ. The values for the initial and final gap widths are the same for all the curves in Fig. 3: $w_i=316.4$ nm and $w_f=1.512$ nm. This means that increasing taper angle θ results in decreasing its length L, and this leads to smaller dissipative losses. In the absence of dissipation, GOA gives no dependence of the relative plasmon intensity on taper angle (dashed line in Fig. 3). This is because GOA neglects the reflective losses, and this is correct only for small taper angles $\theta<\theta_{c1}\approx 7°$.[19] This is the reason for substantial discrepancies between the FDTD and GOA curves for both the cases with and without dissipation at taper angles $\theta>10°$ (Fig. 3). On the other hand, if $\theta<10°$, good agreement between the FDTD and GOA results can be seen (Fig. 3). This is again in agreement with the applicability conditions for GOA derived in Ref. 19.

Another important aspect that follows from Fig. 3 is that the FDTD dependence in the presence of dissipation suggests that there exists an optimal taper angle $\theta_{\text{opt}}\approx 13.5°$ (see circles in Fig. 3) at which the relative plasmon intensity is maximal: $|H_{\text{opt}}|^2/|H_0|^2\approx 21.8$. Note that it is not possible to obtain this optimal angle in GOA—compare circles and squares in Fig. 3. This is because the optimal taper angle is determined by the competition of decreasing dissipative losses and increasing reflective losses when θ is increased (see above). It is clear that θ_{opt} is a function of the wave frequency and permittivities of the metal and the dielectric filling the gap. For example, increasing dissipation (i.e., increasing imaginary part of the permittivity) in the metal results in increasing optimal taper angle.

A taper with the optimal angle works as an optimal adaptor between the waveguides. It enables the most effective energy coupling between two gap plasmon waveguides of different widths. For example, at the optimal taper (i.e., at $\theta=\theta_{\text{opt}}\approx 13.5°$) in the considered structure, highly efficient coupling of gap plasmons from the 316.4 nm waveguide into the 1.512 nm nanowaveguide (or nanofocusing into this narrow region) with the ≈2,200% enhancement of the energy density can be achieved by the tapered structure whose length is only ≈1.3 μm. Increasing taper angle above θ_{opt} results in further reduction of the adaptor length and may still correspond to a significant enhancement of the plasmon field in the narrow waveguide. For example, if $\theta\approx 57.9°$ the increase in the energy density in the plasmon at the end of the taper (at the beginning of the narrow waveguide) is ≈850% with the taper length of ≈0.29 μm.

In summary, this letter presents the numerical FDTD analysis of adiabatic and nonadiabatic nanofocusing of plasmons in tapered nanogaps between two identical metallic media. The analysis was compared with the previously developed approximate theory of adiabatic nanofocusing in metal V grooves,[19] providing good agreement of the approximate and rigorous results for taper angles satisfying the applicability condition for the approximate theory.[19] At the same time, it is also demonstrated that in the nonadiabatic regime of nanofocusing, reflections of plasmons in the focusing structure play a significant role, resulting in the existence of an optimal taper angle for achieving the maximal local field enhancement.

The obtained results will be important for effective delivery of electromagnetic energy to the nanoscale, including nanooptical devices and waveguides, quantum dots, single molecules, etc. In addition, optimal adaptors between different subwavelength plasmonic waveguides were suggested and analyzed.

The authors gratefully acknowledge support from the Japan Society for the Promotion of Science and the High Performance Computing Division at the Queensland University of Technology.

[1] S. A. Maier, P. G. Kik, H. A. Atwater, S. Meltzer, E. Harel, B. E. Koel, and A. A. G. Requicha, Nat. Mater. **2**, 229 (2003).
[2] J. R. Krenn, Nat. Mater. **2**, 210 (2003).
[3] J. Takahara and T. Kobayashi, Opt. Photonics News **15**, 55 (2004).
[4] D. F. P. Pile and D. K. Gramotnev, Opt. Lett. **29**, 1069 (2004).
[5] D. F. P. Pile and D. K. Gramotnev, Appl. Phys. Lett. **86**, 161101 (2005).
[6] D. F. P. Pile and D. K. Gramotnev, Opt. Lett. **30**, 1186 (2005).
[7] D. K. Gramotnev and D. F. P. Pile, Appl. Phys. Lett. **85**, 6323 (2004).
[8] S. Kawata, *Topics in Applied Physics* (Springer, Berlin, 2001), Vol. 81.
[9] W. Srituravanich, N. Fang, C. Sun, Qi. Luo, and X. Zhang, Nano Lett. **4**, 1085 (2004).
[10] K. Kneipp, Y. Wang, H. Kneipp, L. T. Perelman, I. Itzkan, R. R. Dasari, and M. S. Feld, Phys. Rev. Lett. **78**, 1667 (1997).
[11] S. Nie and S. R. Emory, Science **275**, 1102 (1997).
[12] R. Hillenbrand, T. Taubner, and F. Kellmann, Nature (London) **418**, 159 (2002).
[13] B. Pettinger, B. Ren, G. Picardi, R. Schuster, and G. Ertl, Phys. Rev. Lett. **92**, 096101 (2004).
[14] T. Ichimura, N. Hayazawa, M. Hashimoto, Y. Inouye, and S. Kawata, Phys. Rev. Lett. **92**, 220801 (2004).
[15] Kh. V. Nerkararyan, Phys. Lett. A **237**, 103 (1997).
[16] A. J. Babadjanyan, N. L. Margaryan, and Kh. V. Nerkararyan, J. Appl. Phys. **87**, 3785 (2000).
[17] H. Gao, H. Shi, C. Wang, C. Du, X. Luo, Q. Deng, Y. Lv, X. Lin, and H. Yao, Opt. Express **13**, 10795 (2005).
[18] M. I. Stockman, Phys. Rev. Lett. **93**, 137404 (2004).
[19] D. K. Gramotnev, J. Appl. Phys. **98**, 104302 (2005).
[20] H. Miyazaki and Y. Kurokawa, Phys. Rev. Lett. **96**, 097401 (2006).
[21] J. A. Dionne, L. A. Sweatlock, H. A. Atwater, and A. Polman, Phys. Rev. B **73**, 035407 (2006).
[22] D. F. P. Pile, T. Ogawa, D. K. Gramotnev, Y. Matsuzaki, K. C. Vernon, T. Okamoto, M. Haraguchi, and M. Fukui, Appl. Phys. Lett. **87**, 261114 (2005).
[23] G. Veronis and S. Fan, Opt. Lett. **30**, 3359 (2005).
[24] L. Liu, Z. Han, and S. He, Opt. Express **13**, 6645 (2005).
[25] I. A. Larkin, M. I. Stockman, M. Achermann, and V. I. Klimov, Phys. Rev. B **69**, 121403(R) (2004).
[26] A. Liebsch, Phys. Rev. Lett. **54**, 67 (1985).
[27] D. F. P. Pile, Appl. Phys. B: Lasers Opt. **81**, 607 (2005).
[28] G. Mur, IEEE Trans. Electromagn. Compat. **40**, 100 (1998).